Spin–orbit effects in quantum mechanical rate constant calculations for the F+H 2 →HF+H reaction

F. J. Aoiz, L. Bañares, and J. F. Castillo

Citation: The Journal of Chemical Physics **111**, 4013 (1999); doi: 10.1063/1.479703
View online: http://dx.doi.org/10.1063/1.479703
View Table of Contents: http://scitation.aip.org/content/aip/journal/jcp/111/9?ver=pdfcov
Published by the AIP Publishing

Spin–orbit effects in quantum mechanical rate constant calculations for the $F+H_2 \rightarrow HF+H$ reaction

F. J. Aoiz, L. Bañares, and J. F. Castillo[a)]
Departamento de Química Física, Facultad de Química, Universidad Complutense, 28040 Madrid, Spain

(Received 11 May 1999; accepted 3 June 1999)

Exact and approximate quantum mechanical calculations of reaction probabilities and cumulative reaction probabilities have been carried out for the $F+H_2$ reaction on the *ab initio* adiabatic potential energy surfaces by Stark and Werner (SW) and by Hartke, Stark, and Werner (HSW), the latter including spin–orbit corrections in the entrance channel. These data have been employed to obtain thermal rate constants for the title reaction in the temperature range 200–700 K. The exact and approximate results have been compared with experimental determinations and previous theoretical predictions. In particular, the reaction probabilities obtained on the HSW surface are found to be in very good agreement with recent calculations by Alexander *et al.* [J. Chem. Phys. **109**, 5710 (1998)] based on the exact treatment of spin–orbit and Coriolis coupling for this system. However, the rate constants calculated on the HSW PES are systematically lower than the experimental values, which indicates that the height of the adiabatic potential energy surface is too high. Furthermore, an estimate of cross sections from the reaction probabilities calculated by Alexander *et al.* shows that the contribution to the low temperature rate constants from spin–orbit excited $F(^2P_{1/2})$ atoms through nonadiabatic channels is very small and, thus, nonadiabatic effects are not sufficient to bring the calculated rate constants to a better agreement with the experimental measurements. © *1999 American Institute of Physics.* [S0021-9606(99)00533-4]

I. INTRODUCTION

The reaction of F atoms with H_2 molecules has become one of the most studied elementary chemical reactions, both experimentally and theoretically (for recent reviews see Refs. 1–3). The molecular beam experiments carried out in the 1980s by the group of Lee[4,5] made of this reaction a case example for text books on reaction dynamics.[6–8] These cornerstone experiments have been followed by others in which the ultimate rovibrational resolution of the products have been reached. Among the most important contributions to the experimental study of the dynamics of this reaction in the last years, we should mention the molecular beam experiments by the group of Toennies on the $F+D_2$ isotopic variant of the reaction,[9–15] the photodetachment experiments of the FH_2^- ion of Neumark and co-workers,[16,17] and the very recent studies by the groups of Nesbitt[18,19] and Keil[20,21] on the $F+H_2$ reaction. On the theoretical side, the advent of high quality *ab initio* calculations by Truhlar and co-workers[22,23] and by Werner and co-workers[24] during the 1990s have allowed, for the first time, the reproduction of most of the experimental observables by exact quantum mechanical (QM)[1,25,26] reactive scattering and, to a lesser extent, by quasiclassical trajectory (QCT)[27–29] calculations, at an unprecedented level of detail. In particular, the QM calculations on the, nowadays widely used, *ab initio* potential energy surface (PES) by Stark and Werner (hereafter, SW)[24] have permitted an almost perfect simulation of the molecular beam measurements in the form of laboratory angular distributions and time-of-flight spectra of the product molecule[30,31] and of the photodetachment experiments of Neumark and co-workers.[17]

A critical review of literature data on the kinetics of the $F+H_2$ system has been reported recently by Persky and Kornweitz.[32] In this work, the authors recommended Ahrrenius functionalities for the temperature dependence of thermal rate constants of the $F+H_2$ and $F+D_2$ reactions based on the available experimental measurements.[33–35] Rosenman *et al.* have performed QM calculations on the SW PES employing a negative imaginary potential plus coupled-states method[36] to obtain the collision energy dependence of the integral cross sections for the $F+H_2(j=0-3)$ and $F+D_2(j=0-3)$ reactions, and from them the thermal rate constants. The theoretical rate coefficients and kinetic isotope effect were found in general good agreement with the experimental results. Very recently, Wang *et al.*[37] have carried out exact and approximate QM calculations of rate constants for the $F+H_2$ reaction on the SW PES from the integral of the flux–flux autocorrelation function. They found that their exact and approximate (based on the principal axis/helicity-conserving approximation) thermal rate constants were somewhat smaller than those obtained by Rosenman *et al.* and most of the experimental determinations. No other QM calculations on rate constants for the title reaction on the SW PES have been published thus far.

One of the most interesting aspects of this reaction, which is attracting a great deal of attention in the last few years, is the possibility of reaction from the two spin–orbit electronic states of the F atom, i.e., $^2P_{3/2}$ and $^2P_{1/2}$, which are split by 50.1 meV (1.15 kcal mol^{-1}). There are three possible PESs, labeled $1\,^2A'$, $1\,^2A''$ and $2\,^2A'$ in C_s sym-

a)Corresponding author. Electronic mail: jfc@legendre.quim.ucm.es

metry (corresponding to $^2\Sigma_{1/2}$, $^2\Pi_{3/2}$, and $^2\Pi_{1/2}$ in the $C_{\infty v}$ symmetry). Only the $1\,^2A'$ surface correlates the $F(^2P_{3/2})+H_2(^1\Sigma)$ reagents with the ground state products $H(^2S)+HF(^1\Sigma)$, while the $1\,^2A''$ correlates with excited products $H(^2S)+HF(^1\Pi)$, which are not energetically accesible at the collision energies interesting for reaction dynamics. The spin–orbit excited channel $F(^2P_{1/2})+H_2$ correlates exclusively with the excited products through the $2\,^2A'$ surface. Therefore, of the three surfaces commented on, only the $1\,^2A'$ allows the reaction to occur adiabatically. The most immediate influence of the first electronically excited PES ($2\,^2A'$) would be a small perturbation of the lowest adiabatic PES via spin–orbit coupling.

Hartke and Werner have produced a new *ab initio* PES (hereafter HSW), in which spin–orbit corrections were added in the entrance channel of the adiabatic SW PES.[38] The main consequence of the spin–orbit coupling was to increase the height of the barrier on the ground adiabatic $^2\Sigma_{1/2}$ spin–orbit surface relative to the value on the spin-free $^2\Sigma$ SW PES by 0.38 kcal mol^{-1}, leaving the shape in both the transition state region and product valley unchanged with respect to the SW PES. In addition, the height of the van der Waals well in the entrance valley decreased in the HSW PES (0.18 kcal mol^{-1} in comparison with 0.37 kcal mol^{-1} in the SW PES). Using this new HSW PES and a new *ab initio* surface for the anionic species FH_2^-. Hartke and Werner[38] found that the agreement between time-dependent quantum calculations of FH_2^- photoelectron spectra and the photodetachment experiments of Neumark and co-workers was better in comparison with earlier simulations based on the spin–orbit free SW surface.[24] Moreover, it has been suggested recently[1] that dynamical calculations on a spin-orbit corrected adiabatic PES would explain the (small) remaining discrepancies between theory and experiment. With this aim, exact QM and QCT dynamical calculations on the SW and HSW PESs have been performed recently by Castillo *et al.*[31] to simulate the molecular beam experimental results of Lee and co-workers[4,5] and of Keil and co-workers.[20,21] In this work, it has been found, however, that the performance of the HSW PES was, in general, worse than that of the SW PES in reproducing the experimental observables.[31]

A major breakthrough in the theoretical treatment of this reaction has been achieved very recently by Alexander *et al.*[39] They have carried out for the first time a full *ab initio* calculation of the complete set of diabatic PESs and spin–orbit terms for this system. The fitted surfaces and couplings have been used to perfom exact time-independent quantum scattering calculations of reaction transition probabilities taking into account the spin–orbit and Coriolis couplings for the $F(^2P_{3/2,1/2})+H_2(v=0,j=0,1)$ reactions. Thus far, only calculations of reaction probabilities have been performed for total angular momentum (electronic plus nuclear) $J=1/2$. The main conclusion of this work was that reactivity from $F(^2P_{1/2})$ atoms represents less than 10% of that from $F(^2P_{3/2})$, and that the overall features of the scattering can be well represented by calculations on the lowest electronic PES.

Recently, Matzkies and Manthe[40] have proposed a simple correction in the electronic partition function of the reagents in those cases in which there is spin–orbit splitting in order to calculate rate constants on an adiabatic PES constructed without considering the spin–orbit coupling. Usually, the reagent electronic partition function is calculated taking the origin of energy in the ground spin–orbit state; however, in the case in which no spin–orbit correction has been included in the PES, it seems more reasonable to assume that the PES correlates asymptotically to the energy of the open shell reagent without spin–orbit splitting. Thus, the asymptotic energy would correspond to the average energy of the spin–orbit split state of the reagent. This change effectively increases the height of the barrier. Since for the $F+H_2$ reaction there are *ab initio* PESs with and without spin–orbit correction (HSW and SW, respectively), QM calculations of rate constants on both PES will offer a good opportunity to assess the adequacy of the above mentioned correction.

In this paper we have performed exact and approximate QM reaction probability and cumulative reaction probability calculations at selected values of the total angular momentum J on the both the SW and HSW PESs. These results have been used to obtain thermal rate constants with the aim of clarifying the importance of the spin–orbit coupling and the possibility of nonadiabatic effects for this reaction.

The paper is structured as follows: Section II presents the QM methods employed to calculate exact and adiabatic rotation approximate (ARA) reaction probabilities and cumulative reaction probabilities. The J-shifting approximations used to obtain thermal rate constants from the exact cumulative reaction probabilities calculated at total angular momenta $J=0$ and $J=1$ are also described. The results and discussion are presented in Secs. III and IV, respectively, and Sec. V is dedicated to summarize the main conclusions.

II. THEORETICAL METHODS

A. Exact quantum mechanical method

The thermal rate coefficient $k(T)$ can be written as

$$k(T)=\sum_{J=0}(2J+1)k^J(T), \tag{1}$$

where $k^J(T)$, the specific rate constant for total angular momentum J, is given by

$$k^J(T)=\frac{Z_{\rm elec}(T)\int_0^\infty dE\,N^J(E)e^{-E/k_BT}}{h\Phi_{\rm rel}(T)Q_{\rm int}^{H_2}(T)}. \tag{2}$$

In Eq. (2), $Q_{\rm int}^{H_2}(T)$ is the coupled nuclear-rovibrational partition function of H_2 and $\Phi_{\rm ref}(T)$ is the relative translational partition function of $F(^2P)$ with respect to H_2 per unit volume. $Z_{\rm elec}(T)$ is the ratio of the electronic partition function of the transition state divided by the product of the electronic partition function of $F(^2P_{3/2,1/2})$ and H_2, which for this system is given by

$$Z_{\rm elec}(T)=2/(4+2e^{-\Delta/k_BT}) \tag{3}$$

and $\Delta=50.1$ meV(1.15 kcal mol^{-1}) is the F atom $^2P_{1/2}$–$^2P_{3/2}$ splitting. In Sec. IV, the modified electronic partition function for the F atom as proposed by Matzkies and

Manthe[40] will be discussed. $N^J(E)$ in Eq. (2) is the total cumulative reaction probability (CRP) given by

$$N^J(E)=\sum_{vjK}\sum_{v'j'K'}P^J_{vjK\to v'j'K'}(E), \tag{4}$$

where $P^J_{vjK\to v'j'K'}(E)$ is the reaction probability from reactants with initial vibrational, rotational, and helicity quantum numbers v, j, K to products with final vibrational, rotational, and helicity quantum numbers v', j', K'. These probabilities are calculated from the square of the scattering matrix, $|S^J_{\alpha' v'j'K',\alpha vjK}|^2$, where α' labels the HF+H product arrangement and α the F+H_2 reagent arrangement. As pointed out by Wang *et al.* in their previous work on rate constant calculations for the Cl+H_2 (Ref. 41) and F+H_2 (Ref. 37) reactions, one only needs to calculate $k^J(T)$ at a modest number of widely spaced values of J and interpolate accurately to carry out the sum of Eq. (1). Furthermore Eq. (1) can be rewritten as

$$k(T)=\sum_{J=0}(2J+1)\sum_{K=-J}^{J}k^{JK}(T), \tag{5}$$

where K is the projection of the total angular momentum J onto the body-fixed z axis of the reactants. Notice that $k^{JK}(T)$ includes all K' contributions, K' being the projection of J in the product arrangement.

In this work we have performed exact calculations of CRPs at several selected values of J and for values of $K \leqslant K_{\max}$ (see below), and with them we have calculated the specific $k^{JK}(T)$ using Eq. (2). The values of $k^{JK}(T)$ so obtained were then used to calculate $k(T)$ according to Eq. (5) by linear interpolations.

The QM reactive scattering matrix has been calculated using a coupled-channel hyperspherical coordinate method, which has been employed previously in scattering calculations for the F+H_2,[25,31] F+HD,[26] and H+D_2 reactions.[42,43] Converged reaction probabilities and CRPs have been calculated at total angular momenta $J=0,1,2,6,20$ for the F(^2P) $+p-H_2$ and F(^2P)$+o-H_2$ reactions on the SW PES using a basis set including all F(^2P)+H_2 and HF+H channels with diatomic energy levels up to $E_{\max}\leqslant 2.5$ eV and rotational quantum numbers up to $j_{\max}\leqslant 16$. A total of 500 energies have been calculated for each reaction between 0.2682 eV and 1.0157 eV for the F(^2P)$+p-H_2$ reaction and between 0.2829 eV and 1.0314 eV for the F(^2P)$+o-H_2$ reaction. Using this basis set, it has been found that the CRPs are converged to better than 1% for $J=0$, For $J>0$, angular basis functions with helicities up to $K_{\max}=4$ for the reactant and product arrangements have been retained. In a previous work,[31] it was found that well converged state-to-state reaction probabilities were obtained by retaining K values up to 4 for $J>0$ at collision energies up to 0.16 eV. Furthermore, as it will be shown below, the contribution to $k(T)$ from specific $k^{JK}(T)$ with $K>4$ is very small. Wang *et al.*[37] also found that a value of $K_{\max}=4$ was adequate to obtain converged results. The size of the basis sets employed in these calculations is given in Table I. For the HSW PES, the exact QM calculations have been performed only at $J=0$ and $J=1$ using the same basis set as for the SW PES.

TABLE I. Size of the basis set employed in the exact and ARA QM scattering calculations for the F+H_2 reaction on both the SW and HSW PESs.

J	Reaction	Diatomic parity	Triatomic parity	Number of channels
0	F+$p-H_2$	$(-1)^j=1$	$(-1)^p=(-1)^J$	184
0	F+$o-H_2$	$(-1)^j=-1$	$(-1)^p=(-1)^J$	181
1	F+$p-H_2$	$(-1)^j=1$	$(-1)^p=(-1)^J$	170
1	F+$p-H_2$	$(-1)^j=1$	$(-1)^p=(-1)^{J+1}$	354
1	F+$o-H_2$	$(-1)^j=-1$	$(-1)^p=(-1)^J$	172
1	F+$o-H_2$	$(-1)^j=-1$	$(-1)^p=(-1)^{J+1}$	353
$\geqslant$4, even	F+$p-H_2$	$(-1)^j=1$	$(-1)^p=(-1)^J$	800
$\geqslant$4, even	F+$p-H_2$	$(-1)^j=1$	$(-1)^p=(-1)^{J+1}$	616
$\geqslant$4, odd	F+$p-H_2$	$(-1)^j=1$	$(-1)^p=(-1)^J$	616
$\geqslant$4, odd	F+$p-H_2$	$(-1)^j=1$	$(-1)^p=(-1)^{J+1}$	800
$\geqslant$4, even	F+$o-H_2$	$(-1)^j=-1$	$(-1)^p=(-1)^J$	795
$\geqslant$4, even	F+$o-H_2$	$(-1)^j=-1$	$(-1)^p=(-1)^{J+1}$	614
$\geqslant$4, odd	F+$o-H_2$	$(-1)^j=-1$	$(-1)^p=(-1)^J$	614
$\geqslant$4, odd	F+$o-H_2$	$(-1)^j=-1$	$(-1)^p=(-1)^{J+1}$	795

B. *J*-shifting approximations

The *J*-shifting approximation[44] has been applied to obtain thermal rate constants from the accurate CRP calculated at $J=0$ on both the SW and HSW PESs. Within this approximation, the thermal rate constant is given by

$$k(T)=k^{J=0}(T)Q_{JS}(T), \tag{6}$$

where $Q_{JS}(T)$ is the transition state rotational partition function given by

$$Q_{JS}(T)=\sum_{J=0}(2J+1)\sum_{K=-J}^{J}e^{-E_{JK}/k_BT}. \tag{7}$$

In the bent transition state of the SW and HSW PESs (see Table I of Ref. 31), the moments of inertia are $I_A^{\ddagger}\approx I_B^{\ddagger} > I_C^{\ddagger}$ (nearly an oblate symmetric top), and, therefore, the corresponding rotational energy levels can be approximated by[45]

$$E_{JK}=\tfrac{1}{2}(A^{\ddagger}+B^{\ddagger})J(J+1)+[C^{\ddagger}-\tfrac{1}{2}(A^{\ddagger}+B^{\ddagger})]K^2, \tag{8}$$

where the rotational constants for the SW PES are $A^{\ddagger}=2.82\,\mathrm{cm}^{-1}$, $B^{\ddagger}=2.90\,\mathrm{cm}^{-1}$, and $C^{\ddagger}=98.08\,\mathrm{cm}^{-1}$, and for the HSW PES are $A^{\ddagger}=2.80\,\mathrm{cm}^{-1}$, $B^{\ddagger}=2.88\,\mathrm{cm}^{-1}$, and $C^{\ddagger}=96.99\,\mathrm{cm}^{-1}$.

The rate constant for $J=0$, $k^{J=0}(T)$, is calculated from a spline fit of the accurate CRP at $J=0$ using Eq. (2).

An alternative *J*-shifting procedure can be obtained using the accurate CRPs calculated at $J=0$ and $J=1$. The $J=0$ CRP contains only contributions for even bend states of the transition state, whereas for $J>0$ both even and odd bend states contribute. Thus, it has been found that *J* shifting from the exact results at $J=1$ constitutes a better approximation.[46] As pointed out by Wang and Bowman,[46] this would be a special case of the extension of the *J*-shifting approximation proposed by Truhlar and co-workers,[47] in which the *J* shifting is performed from a higher value of *J*, thus including more bending states of the transition state. In the present case, we have assumed that for $J>1$ the $N^{JK}(E)$ can be shifted as follows:

$$N^{J0}(E)=N^{10}(E+E_{10}-E_{J0}),$$
$$N^{JK\neq 0}(E)=N^{11}(E+E_{11}-E_{JK}), \tag{9}$$

where N^{10} and N^{11} are the CRPs for $J=1$, $K=0$ and $J=1$, $K=1$, respectively.

Equation (5) can be rewritten as

$$k(T)=k^{00}(T)+k^{10}(T)\times e^{E_{10}/k_BT}\left[3+\sum_{J=2}(2J+1)e^{E_{J0}/k_BT}\right]+k^{11}(T)\times e^{E_{11}/k_BT}\left[6+\sum_{J=2}\sum_{K=-J,\neq 0}^{J}(2J+1)e^{E_{JK}/k_BT}\right]. \tag{10}$$

As above, the specific $k^{00}(T)$, $k^{10}(T)$, and $k^{11}(T)$ are calculated from the corresponding CRPs using Eq. (2).

The *J*-shifting approximations have been as well used to calculate the collision energy ($E_{\rm col}$) dependence of the reaction cross section for a specific v, j initial state, $\sigma_{vj}(E_{\rm col})$, from the accurate reaction probabilities at $J=0$ and $J=1$, $P_{vj}^{J=0}(E)$ and $P_{vj}^{J=1}(E)$, for the $F(^2P)+H_2(v=0,j=0,1)$ reactions. For the *J*-shifting from $J=0$ one has

$$\sigma_{vj}(E_{\rm col})=\frac{\pi}{k_{vj}^2}\sum_J(2J+1)P_{vj}^{J=0}(E-E_{J0}) \tag{11}$$

where $k_{vj}=\sqrt{2\mu_{FH_2}E_{\rm col}}/\hbar$.

Analogously, for the *J*-shifting from $J=1$,

$$\sigma_{vj}(E_{\rm col})=\frac{\pi}{k_{vj}^2}\left[P_{vj}^{J=0}(E)+\sum_{J\geqslant 1}(2J+1)\times P_{vj}^{J=1}(E+E_{10}-E_{J0})+\sum_{J\geqslant 1}(2J+1)\times\sum_{K=-J,K\neq 0}^{J}P_{vj}^{J=1}(E+E_{11}-E_{JK})\right]. \tag{12}$$

In Eqs. (11) and (12), the reaction probability $P_{vj}^J(E)$ is given by

$$P_{vj}^J(E)=\frac{1}{2j+1}\sum_{v'j'}\sum_{KK'}|S^J_{\alpha' v'j'K',\alpha vjK}|^2. \tag{13}$$

The E_{JK} which appears in Eqs. (9)–(12) are calculated from Eq. (8) and $E=E_{\rm col}+E_{\rm int}^{v,j}$ where $E_{\rm int}^{v,j}$ is the internal energy corresponding to $H_2(v=0,j=0,1)$.

In addition, we have applied the *J*-shifting approximation to obtain the excitation functions for the $F(^2P_{1/2})+H_2(v=0,j=0)$ and $F(^2P_{3/2})+H_2(v=0,j=0)$ reactions from the $P_{v=j=0,j_a=1/2,3/2}^{J=1/2}(E)$ reaction probabilities reported by Alexander *et al.*, which were calculated as[39]

$$P_{vj,j_a}^J(E)=\frac{1}{(2j+1)(2j_a+1)}\sum_{v',j',k,\omega,\eta}|S^{JK}_{v'j',jkj_a\omega\eta}|^2, \tag{14}$$

where the summation extends to all the final v',j' states, the quantum numbers k and ω, which are the projections of j and j_a onto the entrance channel body-fixed frame, respectively, and the parity index η.[39]

In a similar fashion as that used by Schatz *et al.*[48] for the $Cl(^2P)+HCl$ reaction, we have for the $F(^2P_{j_a=1/2,3/2})+H_2(v=0,j=0)$ reactions

$$\sigma_{vj,j_a}(E_{\rm col})=\frac{\pi}{k_{vj}^2}\sum_J(2J+1)\times P_{vj,j_a}^{J=1/2}(E+E_{J=1/2}-E_J-E_{j_a}),\quad \text{with } J=\tfrac{1}{2},\tfrac{3}{2},\tfrac{5}{2},\cdots, \tag{15}$$

where $E_J=1/2(A^{\ddagger}+B^{\ddagger})J(J+1)$ and E_{j_a} is zero and 50.1 meV, for the reaction with $F(^2P_{j_a=3/2})$ and $F(^2P_{j_a=1/2})$ atoms, respectively. Notice that in doing so the origin of the total energy scale is taken at the minimum of the entrance channel for the reaction with $F(^2P_{j_a=3/2})$.

The corresponding specific rate constants $k_{vj}(T)$ are calculated from the excitation functions $\sigma_{vj}(E_{\rm col})$ using the usual formula

$$k_{vj}(T)=\sqrt{\frac{8k_BT}{\pi\mu}}(k_BT)^{-2}\int_0^{\infty}dE_{\rm col}E_{\rm col}\sigma_{vj}(E_{\rm col})e^{-E_{\rm col}/k_BT}. \tag{16}$$

Notice that in order to compare the specific rate constants $k_{vj}(T)$ obtained from Eq. (16) with the thermal rate constants calculated using Eqs. (2) and (5), the reaction cross sections given by Eqs. (11) and (12) must be divided by 2 to account for the fact that reaction takes place exclusively on only the lowest ($1\,^2A'$) of the two PESs correlating with the ground state reagents $F(^2P_{3/2})+H_2$. In the case of the nonadiabatic calculations of Alexander *et al.*, this factor of 1/2 should be unnecessary. However, the results of Ref. 39 were presented in a way that they could be directly comparable with the adiabatic calculations, and, therefore, the $P_{vj,j_a=3/2}^{J=1/2}(E)$ given in Ref. 39 must be also divided by 2. In what follows, the results for reaction probabilities and cross sections will not include the factor of 1/2, whereas those of rate constants will include it.

C. Adiabatic rotation approximation

In analogy with the work of Wang *et al.*,[37] we have performed calculations using the principal axis helicity-conserving approximation (PA/HCA), also named adiabatic rotation approximation (ARA).[46,49] Briefly, the ARA method consists in neglecting the Coriolis coupling terms in the total Hamiltonian and substituting the asymmetric top terms of the rotational Hamiltonian by that of a symmetric top rotor.[50] In this way, the external degrees of freedom are decoupled from the internal ones and K is conserved in the reaction thus becoming a good quantum number, i.e., $K=K'$.

The total Hamiltonian in the ARA method is built by adding to the $J=0$ Hamiltonian, $H^{J=0}$, a term which depends parametrically on the internal coordinates describing the rotation of the triatom as a whole. Thus, the Hamiltonian in Jacobi coordinates (r,R,γ) in a given arrangement is given by

$$H^{JK}=H^{J=0}+E_{JK}(r,R,\gamma), \tag{17}$$

where $E_{JK}(r,R,\gamma)$ is the rotational energy of a nearly symmetric top rotor.

$$E_{JK}(r,R,\gamma)=\tfrac{1}{2}[A(r,R,\gamma)+B(r,R,\gamma)][J(J+1)-K^2] + C(r,R,\gamma)K^2 \quad (18)$$

and the rotational constants, A, B, and C are given in terms of the principal moments of inertia I_A, I_B, and I_C, respectively (i.e., $A=\hbar^2/2I_A$, etc.). In the present case,

$$I_C=\tfrac{1}{2}(MR^2+mr^2)-\tfrac{1}{2}[(MR^2)^2+(mr^2)^2 + 2MR^2mr^2\cos 2\gamma]^{1/2},$$
$$I_B=\tfrac{1}{2}(MR^2+mr^2)+\tfrac{1}{2}[(MR^2)^2+(mr^2)^2 + 2MR^2mr^2\cos 2\gamma]^{1/2}, \quad (19)$$
$$I_A=I_B+I_C=MR^2+mr^2,$$

where M and m are the reduced masses of the FH_2 system and H_2 diatom, respectively.

The term E_{JK} in Eq. (15) is essentially a centrifugal potential added to the PES to produce an effective potential on which the reaction dynamics evolve. It should be noted that the ARA calculations have to be performed at fixed values of J and K, each of these calculations requiring the same computational effort than a calculation at $J=0$.

As described in Ref. 50, ARA has been implemented successfully in our coupled-channel hyperspherical coordinate scattering code and the method has been applied to study the F+H_2 and Cl+H_2 reaction dynamics. ARA has shown to be quite reliable to calculate integral cross sections, even at the level of vibrational resolution of the products for these two reactive systems. The main differences found between ARA and exact QM results arose from neglecting the Coriolis coupling. However, it was demonstrated that the separation of internal motions from the overall rotational motion is a good aproximation.[50]

As in Sec. II A, the specific $k^{JK}(T)$ have been obtained from the calculated ARA CRPs for each value of K at several selected values of J, and from them $k(T)$ has been calculated by linear interpolations using Eq. (5). The ARA reactive scattering matrices have been calculated at $J=0$, 1, 2, 6, 15, 20, and 25 with $K=\min(J,K_{\max}=4)$ on both the SW and HSW PESs using the same basis sets as for the exact calculations (see Table I).

III. RESULTS

A. Cumulative reaction probabilities

As shown in the preceding section, the basic dynamical magnitude needed to calculate thermal rate constants is the specific CRP, $N^{JK}(E)$. Figure 1 displays the exact QM CRPs calculated at $J=0$ for the F+p-H_2 and F+o-H_2 reactions on both the SW and HSW PESs. The physical origin of the prominent low energy peaks of the CRPs calculated on the SW PES have been discussed in detail in Refs. 1, 25, and 26. Briefly, the broad peak appearing at the lowest total energies has been associated with the dynamics of the reactive system in the transition state region, whereas the second sharp peak has been assigned to a quasibound resonance state localized

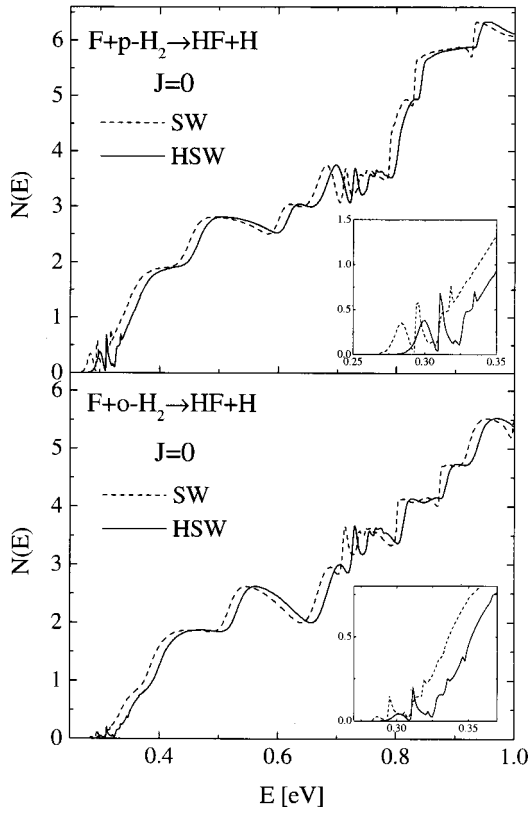

FIG. 1. Cumulative reaction probabilities calculated at $J=0$ on the SW and HSW PESs for the F+$p-H_2$ (top) and F+$o-H_2$ (bottom) reactions.

in the H–HF van der Waals well region. The same double peak structure is also obtained from the calculations on the HSW PES. The staircase like structure at higher total energies is due to adiabatic reaction channels becoming energetically accessible in the transition state as the total energy increases.[51,52] Note that the CRPs calculated on both the SW and HSW PES have the same general structure and the fundamental difference between them is that the CRPs calculated on the HSW PES are shifted towards higher total energies. This is expected since the spin-orbit correction introduced in the HSW PES has the effect of increasing the height of the barrier to reaction by 1/3 of the spin–orbit splitting of the F atom with respect to that of the SW PES, leaving the rest of the PES unchanged. The difference in the van der Waals wells present in the entrance channel of the HSW and SW PESs does not seem to have significant effects on the dynamics of the reaction.

Figure 2 shows the exact and ARA K-resolved CRPs calculated at $J=1$ for the F+p-H_2 and F+o-H_2 reactions on the SW PES. As can be seen, there is an excellent agreement between the exact and ARA calculations. This indicates that the coupling between external and internal degrees of freedom is small for $J=1$, which makes ARA an excellent approximation to the exact calculation for low values of J. Interestingly, for $J=1$ the contributions from initial $K=0$ and $K=1$ are of the same order and the peak structure at low total energies is only present in the CRPs calculated with initial $K=0$.

As the total angular momentum J increases, the agreement between the exact and ARA K-resolved CRPs worsens

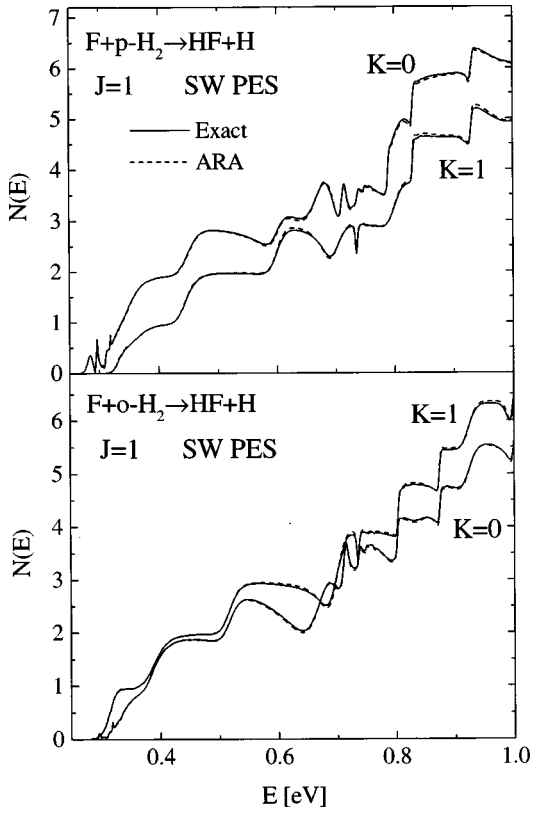

FIG. 2. Exact and ARA cumulative reaction probabilities calculated at $J=1$, $K=0$, 1 on the SW PES for the $F+p-H_2$ (top) and $F+o-H_2$ (bottom) reactions.

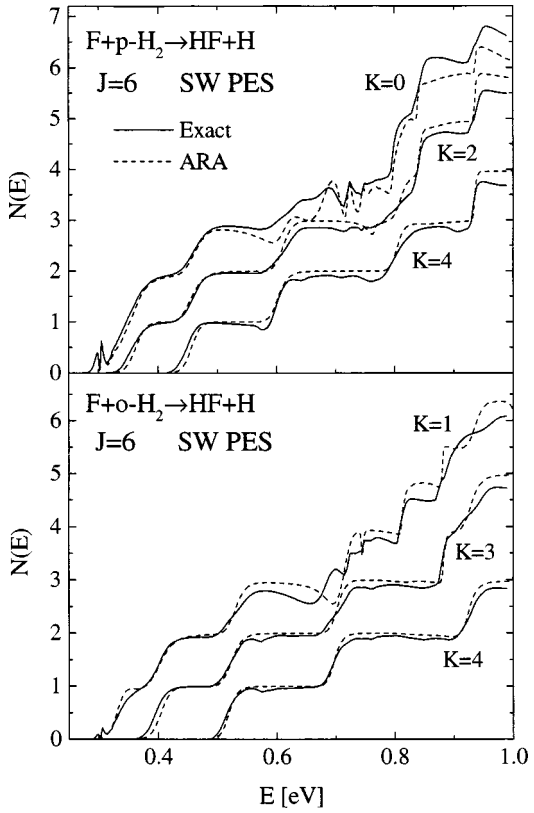

FIG. 3. Exact and ARA cumulative reaction probabilities calculated at $J=6$ and selected values of K on the SW PES for the $F+p-H_2$ (top) and $F+o-H_2$ (bottom) reactions.

significantly due to the increasing importance of the Coriolis coupling terms for larger values of J. Figure 3 illustrates this caveat with respect the ARA method when compared with the exact one for the CRPs calculated on the SW PES at $J=6$ and at some selected values of initial K. As expected, the agreement between the exact and ARA $N^{JK}(E)$ for $J=20$ (not shown) is much worse than that found for $J=6$.

B. Rate constants

Figure 4 displays the dependence of the exact and ARA $k^{JK}(T)$ on J and K for two temperatures (300 K and 500 K) calculated on the SW PES. As can be seen, the data for each temperature can be fitted, in general, to a straight line $\ln k^{JK}=a+bJ(J+1)$, where a and b are the parameters of the fit. Once these parameters have been obtained for each temperature and K value, the thermal rate constant $k(T)$ is obtained in a straightforward manner using Eq. (5). Note that the exact and ARA $k^{JK}(T)$ decreases markedly with K for each value of J and, thus, the use of $K_{\max}=4$ in both the exact and ARA calculations with $J>4$ is a good approximation. Since the calculation of the thermal $k(T)$ using the exact CRPs is based on a limited amount of computations ($J=0,1,6,20$) and on a fit to a linear functionality of the available $k^{JK}(T)$, in what follows we will termed this rate constant as ''exact.''

For a given K value, the differences between the exact and ARA $k^{JK}(T)$ increase with increasing J. Whereas the ARA values are very close to the exact ones for $J=1$, reflecting the good agreement found between the CRPs calculated from the two methods (see Fig. 2), the exact values are, in general, larger than the ARA ones by about 15–25 % at $J=6$ and the differences are as high as 90% at $J=20$, $K=4$ at 300 K. The only exception to this rule occurs for $K=0$, where the ARA $k^{J=20}(T)$ is larger than the exact one. Moreover, for $K=1$ the exact $k^{JK}(T)$ at $J=20$ is larger than that for $K=0$, whereas at $J=6$ the opposite stands. In other words, the slope of the $\ln k^{JK}$ vs $J(J+1)$ straight line functionality is larger for $K=0$ than for $K=1$ in the exact calculation. Actually, the exact calculation shows that as K increases the slopes of the corresponding straight lines become smaller and this fact reflects the increasing importance of the Coriolis coupling with increasing J. In contrast, in the ARA calculations the straight lines obtained for the different K values are, to a good approximation, parallel with the only exception of $K=0$. From the data shown in Fig. 4, it is expected that the ''exact'' $k(T)$ will be somewhat larger than the ARA ones.

Table II compares the present thermal rate constants calculated on the SW PES using the J-shifting approximations (JSA) from $J=0$ and from $J=1$ (hereafter JSA0 and JSA1, respectively), and the ARA and ''exact'' methods. The theoretical results reported by Rosenman *et al.*[36] and Wang *et al.*[37] on the same PES, and the experimental determinations of Refs. 33–35 are also included in the table. Several important conclusions can be drawn from the data listed in Table II. In first place, let us consider the present rate constants obtained using the simpler JSA. It is clear that the JSA

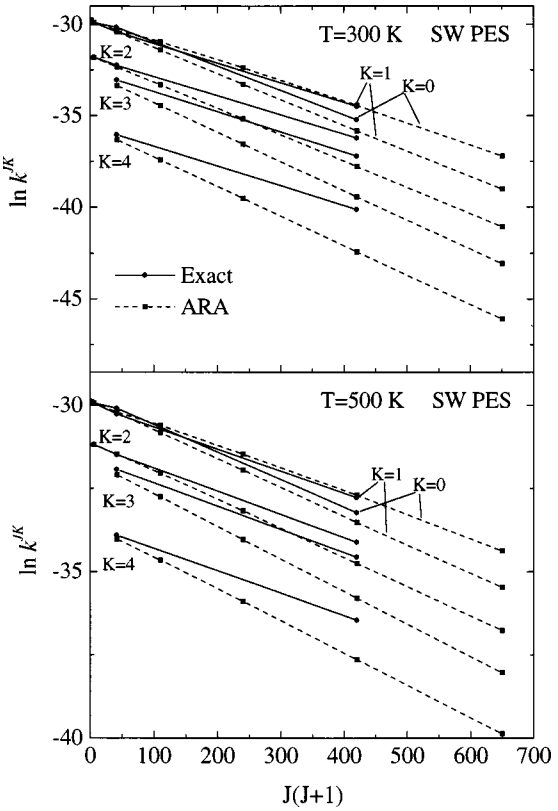

FIG. 4. Exact (circles with solid line) and ARA (squares with dashed line) specific k^{JK} rate constants as a function of $J(J+1)$ at the indicated K values calculated on the SW PES for the F+n−H_2 reaction at 300 K (top) and 500 K (bottom).

from $J=0$ underestimates the rate coefficients in comparison with the ARA and ''exact'' methods and a great improvement is achieved when one makes the shifting from $J=1$. As it was already stated above, this is a consequence of the large contribution to the total $N(E)$ of channels with initial $K=1$. As can be seen, the present JSA1 rate constants are very close to those obtained using the ARA and ''exact'' methods and only at the highest temperatures, the JSA1 $k(T)$ are somewhat larger (about 5% at 700 K). Therefore, the inclusion in the $N(E)$ of contributions from even and odd bend states of the transition state yields JSA rate coefficients in good agreement with those obtained using more exact methods.

It should be noted that our JSA0 rate constants are clearly at variance with those reported by Wang *et al.*[37] on the same SW PES. In fact, their JSA0 rate constants at high temperatures are larger than any of the rate constants calculated with much more accurate methods. The reason for the disagreement could be in the different values of the rotational constants used by Wang *et al.*[37] in comparison with those used in the present work. They reported a rotational constant $B^{\ddagger}=2.340\ \mathrm{cm}^{-1}$, which is significantly smaller than the rotational constants $A^{\ddagger}=2.82\ \mathrm{cm}^{-1}$ and $B^{\ddagger}=2.90\ \mathrm{cm}^{-1}$ calculated in the present work from the bent transition state parameters of the SW PES listed in Table I of Ref. 31. A smaller $B^{\ddagger}$ value would yield a larger $Q_{JS}(T)$ in Eq. (8) and therefore larger $k(T)$. It is not clear why the authors of Ref. 37 used this rotational constant, unless they have calculated $B^{\ddagger}$ using the parameters of the linear saddle point of the SW PES. If one takes the parameters corresponding to that linear saddle point (Table I in Ref. 31) a value of $B^{\ddagger}=2.35\ \mathrm{cm}^{-1}$ is obtained.

The present rate constants calculated on the SW PES using ARA are in excellent agreement with those obtained by Rosenman *et al.*[36] using the negative imaginary potential method plus coupled-states approximation (NIP–CSA). However, they are again in disagreement with the flux–flux autocorrelation function plus PA/HCA results of Wang *et al.*[37] It must be noted as well that the present ''exact'' $k(T)$ are also larger than those reported by Wang *et al.* (about 25% at 300 K).

Table III lists the present JSA0, JSA1 and ARA rate constants calculated on the HSW PES along with the most representative experimental values. All rate constants calculated on the HSW PES are much smaller than the experimental determinations and than the corresponding rate coefficients calculated using the same methods on the SW PES (see Table II). The higher barrier of the adiabatic, spin–orbit corrected, HSW PES in comparison with the SW PES is the origin of the smaller overall reactivity on this PES, reflected in the smaller values of $k(T)$.

TABLE II. Experimental and theoretical thermal rate constants $k(T)$ ($\times 10^{11}\ \mathrm{cm}^3\ \mathrm{s}^{-1}$) for the F+$n$−$H_2$ reaction as a function of temperature. The theoretical $k(T)$ have been calculated on the SW PES.

T(K)	WH[a]	SBA[b]	HBGM[c]	CSA[d]	JSA0[e]	PA/HCA[f]	''Exact'' [g]	JSA0[h]	JSA1[i]	ARA[j]	''Exact'' [k]
200	1.14			1.66				1.26	1.66	1.67	1.85
250	1.76	1.83		2.25				1.70	2.29		
300	2.33	2.48	2.91	2.81	2.52	1.93	2.26	2.20	2.94	2.84	3.11
350	2.89	3.14	3.92	3.35	3.48	2.58		2.72	3.56	3.46	3.71
400			4.85	3.80	4.42	3.27		3.24	4.16	4.02	4.26
450			5.73		5.08	3.74		3.77	4.74	4.55	4.77
500			6.54		5.74	4.16		4.29	5.28	5.06	5.24
600			8.01		7.32	5.27	5.68	5.29	6.29	5.97	6.08
700			9.23		8.62	6.19		6.22	7.21	6.78	6.81

[a]Experimental values from Wurzberg and Houston (Ref. 33).
[b]Experimental values from Stevens *et al.* (Ref. 35).
[c]Experimental values from Heidner *et al.* (Ref. 34).
[d]Theoretical values from Rosenman *et al.* (Ref. 36).
[e–g]Theoretical values from Wang *et al.* (Ref. 37).
[h–k]Present work.

TABLE III. Experimental and theoretical thermal rate constants $k(T)$ ($\times 10^{11}$ cm^3 s^{-1}) for the $F+n-H_2$ reaction as a function of temperature. The theoretical $k(T)$ have been calculated on the HSW PES.

T(K)	WH[a]	SBA[b]	HBGM[c]	JSA0[d]	JSA1[e]	ARA[f]
200	1.14			0.50	0.67	0.63
250	1.76	1.83		0.81	1.11	
300	2.33	2.48	2.91	1.18	1.60	1.51
350	2.89	3.14	3.92	1.60	2.12	1.99
400			4.85	2.04	2.65	2.48
450			5.73	2.51	3.17	
500			6.54	2.97	3.68	3.43
600			8.01	3.90	4.66	4.32
700			9.23	4.80	5.58	5.23

[a]Experimental values from Wurzberg and Houston (Ref. 33).
[b]Experimental values from Stevens *et al.* (Ref. 35).
[c]Experimental values from Heidner *et al.* (Ref. 34).
[d–f]Present work.

Figure 5 depicts the comparison between the present ARA and ''exact'' rate constants calculated on the SW PES and the corresponding ARA values calculated on the HSW PES. In addition, the experimental measurements and the approximate QM calculations by Rosenman *et al.* are also represented in the figure. The present ARA and ''exact'' rate constants calculated on the SW PES are slightly above the experimental data at low temperatures, while at the highest temperatures they are somewhat smaller. The ARA rate constants calculated on the HSW PES are, however, well below all the experimental determinations. At first glance, the comparison with the experimental results at $T \leqslant 300$ K seems to indicate that the SW PES has a barrier which is too low, whereas that of the spin–orbit corrected HSW PES is too high.

IV. DISCUSSION

In all the rate constant calculations made so far, we have employed Eq. (2). In this equation, $Z_{\mathrm{elec}}(T)$ is the ratio of the electronic partition function of the transition state divided by the product of the electronic partition functions of the F atom and the H_2 molecule. In the case of the F atom, the electronic partition function is given by $Z^F_{\mathrm{elec}}(T)=4+2e^{-\Delta/k_BT}$, and Δ corresponds to the F atom $^2P_{1/2}$-$^2P_{3/2}$ splitting. This partition function would correspond to a potential energy surface which asymptotically correlates to the ground spin–orbit state $^2P_{3/2}$ of the F atom. However, as pointed out recently by Matzkies and Manthe,[40] when an adiabatic surface involving open-shell atoms or molecules is calculated without spin–orbit coupling, as it is the case of the SW PES, it seems reasonable to assume that the PES correlates asymptotically to the energy of the atom or molecule without spin–orbit splitting, which, in the present case, would correspond to the average energy of the spin–orbit split ^2P state of the F atom. To take this into account, the corresponding electronic partition function would have to be

$$Z^{\mathrm{F}}_{\mathrm{elec}}(T)=4e^{\Delta/3k_BT}+2e^{-2\Delta/3k_BT}. \tag{20}$$

This equation implicitly assumes that the effect of the spin–orbit coupling is negligible in the transition state region but changes the origin of energy in the reagent asymptote of the PES by $\Delta/3$, a fact which seems to be corroborated by the *ab initio* calculations carried out by Werner and co-workers.[31,38] In any case, the major net effect is to effectively increase the dynamical barrier of the spin-free SW PES by precisely 1/3 of the F-atom spin–orbit splitting. The point which remains to be demonstrated is whether the inclusion of the spin–orbit coupling in the HSW PES with respect to the original SW PES has some dynamical consequences in the calculations of rate constants which are not accounted for by the simple correction to the F-atom electronic partition function.

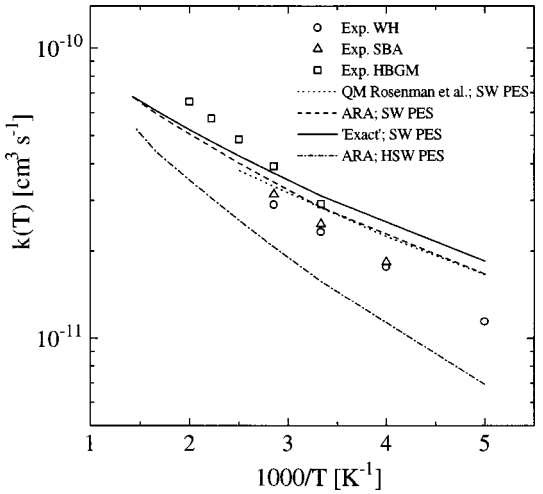

FIG. 5. Arrhenius like plot of the thermal rate constants for the $F+n-H_2$ reaction. Symbols: experimental determinations from Ref. 33 (circles), Ref. 35 (triangles), and Ref. 34 (squares). Dotted line: approximate QM calculations by Rosenman *et al.* on the SW PES (Ref. 36). Dashed and solid lines: present ARA and ''exact'' results on the SW PES. Dashed–dotted line: present ARA results on the HSW PES.

Figure 6 shows the comparison between the ARA $k(T)$ calculated on the HSW PES using the conventional F-atom electronic partition function [Eq. (3)] and the ARA and ''exact'' rate constants calculated on the SW PES using the electronic partition function given by Eq. (20). The ''corrected'' rate constants calculated on the SW PES agree rather well with those obtained on the HSW PES, yielding an Arrhenius-type functionality very similar to that obtained on the HSW PES. Therefore, the results shown in Fig. 6 indicate that the use of a modified electronic partition function as the one given by Eq. (20) is, in principle, a good approximation to calculate rate constants on an adiabatic surface without spin–orbit correction included. Given the discrepancies between the set of experimental determinations of $k(T)$ and the QM values obtained from adiabatic calculations with spin–orbit correction the conclusion to be drawn is that either the barrier of the HSW PES is too high (and, consequently, that of the SW PES when the spin–orbit correction is taken into account), or the nonadiabatic contribution from spin–orbit excited F($^2P_{1/2}$) atoms to the reaction is important enough as to explain the observed differences.

A. Comparison of adiabatic and nonadiabatic reaction probabilities

The next issue for discussion is, therefore, the validity of the dynamical calculations on an adiabatic *ab initio* PES con-

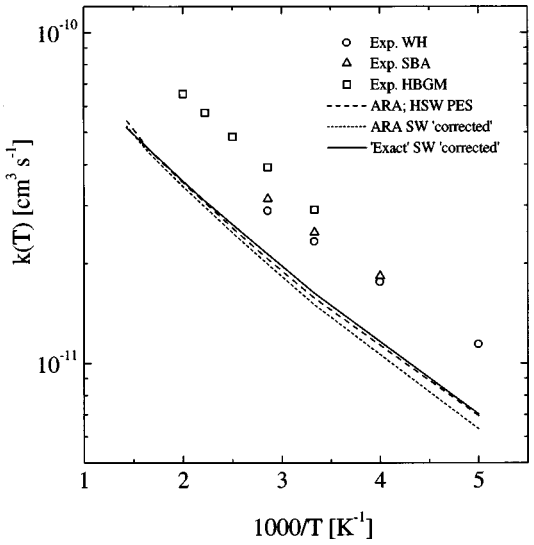

FIG. 6. Arrhenius like plot of the thermal rate constants for the $F+n-H_2$ reaction. Symbols: experimental determinations as in Fig. 5. Dashed line: present ARA results on the HSW PES. Solid and dotted lines: present ARA and ''exact'' corrected results calculated on the SW PES using the electronic partition function given by Eq. (20).

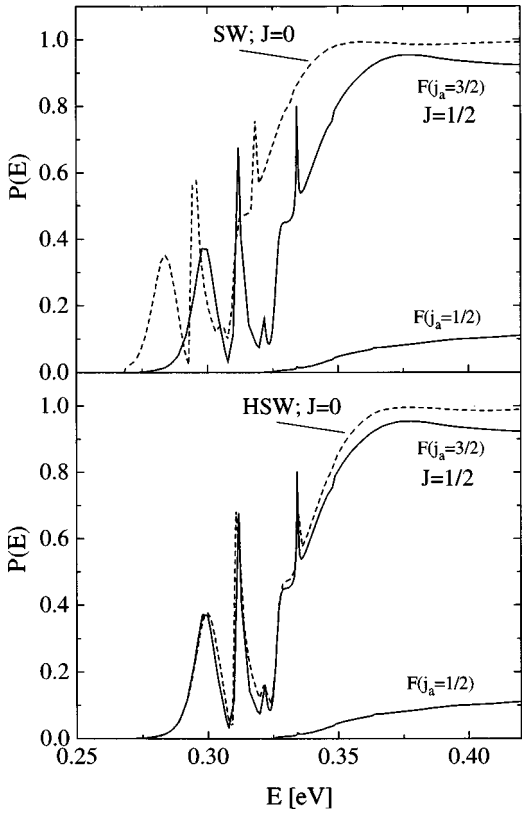

FIG. 7. Reaction probability as a function of the total energy for the $F+H_2(v=0, j=0)$ reaction. The dashed lines correspond to the adiabatic calculations at $J=0$ on the SW PES (top panel) and HSW PES (bottom panel). The solid lines in both panels are the nonadiabatic calculations for the $F(^2P_{j_a=1/2,3/2})+H_2(v=0, j=0)$ reactions reported by Alexander *et al.* (Ref. 39) as indicated.

structed by introducing spin–orbit corrections in the entrance channel, as it is the case of the HSW PES. Thus far, nonadiabatic calculations for the title reaction are restricted to the reaction probabilities calculated for the lowest total (nuclear plus electronic) angular momentum, $J=1/2$, reported by Alexander *et al.*[39] These calculations were performed for the $F(^2P_{1/2})+H_2(v=0, j=0,1)$ and $F(^2P_{3/2})+H_2(v=0, j=0,1)$ reactions using all the diabatic PESs and spin–orbit terms and taking into account the spin–orbit and Coriolis couplings.

Figure 7 shows the comparison between the present reaction probabilities as a function of total energy, $P(E)$, calculated at $J=0$ on the adiabatic SW and HSW PESs for the $F(^2P)+H_2(v=0, j=0)$ reaction and those obtained by Alexander *et al.*[39] for the corresponding reactions with $F(^2P_{1/2})$ and $F(^2P_{3/2})$ atoms for $J=1/2$. In the $P^{J=0}(E)$ calculated on the SW PES, the origin of total energy is taken in the unsplit $F(^2P)$ atom, whereas in the cases of the adiabatic calculations on the HSW PES and of the nonadiabatic calculations reported by Alexander *et al.*, the origin has been taken at the lowest spin–orbit $^2P_{3/2}$ state of the F atom. Notice, however, that in the original reaction probabilities reported by Alexander *et al.* in Ref. 39, the zero of energy was taken at the unsplit $F(^2P)$ in order to compare with the adiabatic results on the SW PES. As can be seen, there is an almost quantitative agreement between the adiabatic calculation on the HSW PES at $J=0$ and the non-adiabatic one at $J=1/2$ for the $F(^2P_{3/2})+H_2(v=0, j=0)$ reaction, whereas the calculation on the SW PES is shifted towards smaller total energies reflecting the lower effective barrier on this adiabatic PES. The reaction probabilities calculated on both the SW and HSW PESs at $J=1$ are practically undistinguishable with those calculated at $J=0$, and are not shown for the sake of clarity. Only at total energies above 0.35 eV the nonadiabatic reaction probabilities for $J=1/2$ and $j_a=3/2$ become slightly smaller than those obtained on the HSW PES for $J=0,1$.

Figure 8 presents the comparison of the reaction probabilities for the $F+H_2(v=0,j=1)$ reaction. The top panel depicts the calculations performed on the SW PES at $J=0$ and $J=1$ and the corresponding nonadiabatic ones. The results obtained on the HSW PES are shown in the lower panel. The calculations at $J=0$ and $J=1$ on the SW PES for the $F(^2P)+H_2(v=0,j=1)$ reaction are shifted towards smaller total energies with respect to the nonadiabatic calculation at $J=1/2$ for the reaction with $F(^2P_{3/2})$ atoms. In contrast, the nonadiabatic calculation for $J=1/2$ and $j=1$, $j_a=3/2$ lies in between the reaction probabilities for $J=0$ and $J=1$, calculated on the HSW PES. This is to be expected given the dependence of the $P(E)$'s with J for $j=1$ in the adiabatic calculations. Notice that the prominent peak which appears at low total energies in the $P(E)$ is located at exactly the same total energy in the adiabatic and nonadiabatic calculations. The comparisons shown in Figs. 7 and 8 indicate that the nonadiabatic calculations for the reaction with $F(^2P_{3/2})$ atoms are in good agreement with those predicted by the adiabatic calculations on the HSW PES, i.e., once the spin–orbit coupling is taken into account.

Although the reactivity of $F(^2P_{1/2})$ seems to be considerably smaller than that of $F(^2P_{3/2})$ at the same total energy, it might be argued that the inclusion of nonadiabatic effects may be sufficient to calculate rate constants in better agreement with the experimental results. Unfortunately, in spite of

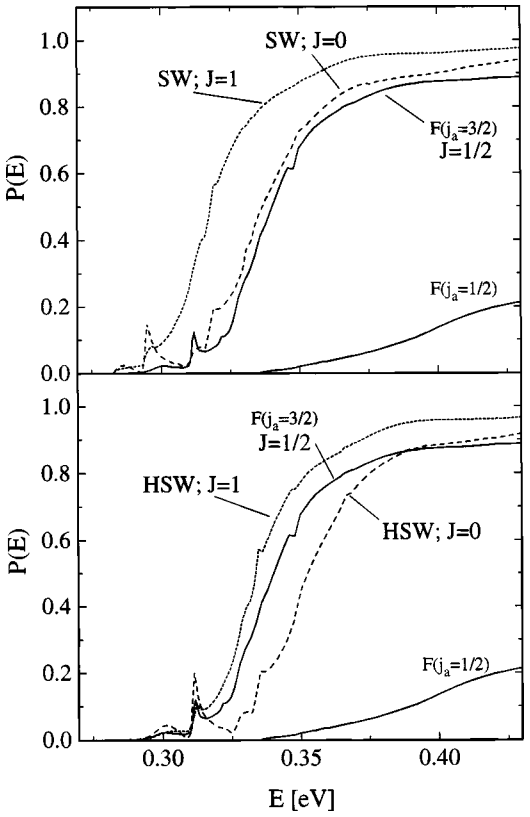

FIG. 8. Same as in Fig. 7 but for the $F+H_2(v=0,j=1)$ reaction. The adiabatic calculations on both the SW and HSW PESs have been carried out at $J=0$ (dashed lines) and $J=1$ (dotted lines). The solid lines correspond to the nonadiabatic calculations taken from Ref. 39.

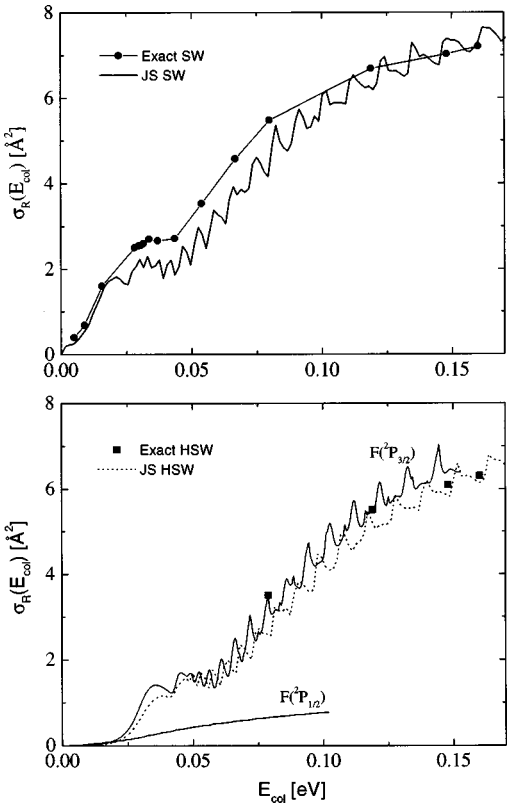

FIG. 9. Top panel: collision energy dependence of the reaction cross section for the $F+H_2(v=0,j=0)$ reaction calculated from the accurate QM reaction probabilities at $J=0$ on the adiabatic SW PES using the *J*-shifting approximation (solid line). For comparison purposes, the accurate results available (Refs. 31 and 53) are depicted as solid circles with solid line. Bottom panel: the solid lines correspond to the excitation functions for the $F(^2P_{1/2,3/2})+H(v=0,j=0)$ reactions calculated using the *J*-shifting approximation from the nonadiabatic reaction probabilities at $J=1/2$ reported by Alexander *et al.*(Ref. 39). The corresponding excitation function calculated on the HSW PES is depicted with a dotted line along with the accurate results (solid squares) available (Ref. 31). All these *J*-shifting excitation functions have been used to calculate the specific rate constants $k_{v=0,j=0}$ using Eq. (16).

the achievements presented in Ref. 39, a full nonadiabatic calculation for all the necessary *J*'s to get reaction cross sections and rate constants has not been performed yet and, certainly, will require a very important computational effort. However, given the acceptable agreement found between the ''exact'' rate constants and those obtained from the application of the *J*-shifting approximation, it might be expected that the use of this latter approximation would serve to obtain a good estimate of cross sections and rate constants for the $F(^2P_{1/2})+H_2(v=0,j=0)$ and $F(^2P_{3/2})+H_2(v=0,j=0)$ reactions from the corresponding reaction probabilities.

B. Comparison of approximate adiabatic and nonadiabatic cross sections and rate constants for the $F+H_2(v=0,j=0)$ reaction

In an attempt to estimate the influence of nonadiabatic effects, we have applied the *J*-shifting approximation to calculate excitation functions for the $F(^2P_{3/2},^2P_{1/2})+H_2(v=0,j=0)$ reactions using Eq. (15) and the reaction probabilities reported by Alexander *et al.*[39] The calculated excitation functions are plotted in Fig. 9. Besides the *J*-shifting excitation functions obtained for the $F(^2P)+H_2(v=0,j=0)$ reaction on the adiabatic SW and HSW PESs are displayed along with exact results.[31,53] Notice that the *J*-shifting approximation values calculated on the SW and HSW PESs are in acceptable agreement with the corresponding exact calculations, and, thus, the method can be used to get reliable estimates of the rate constants for the $F(^2P_{3/2})+H_2(v=0,j=0)$ and $F(^2P_{1/2})+H_2(v=0,j=0)$ reactions.

Since Alexander *et al.* determined reaction probabilities as a function of collision energy up to 0.10–0.15 eV, we can only give reliable rate constants at the lowest temperatures. Using the excitation functions for the $F(^2P_{3/2})$ and $F(^2P_{1/2})$ reactions shown in Fig. 9 and using Eq. (16), the calculated $k_{v=0,j=0}$ rate constants at 200 K are $7.73\times10^{-12}\,cm^3\,s^{-1}$ and $3.59\times10^{-12}\,cm^3\,s^{-1}$, assuming that 100% of the F atoms were in either the 3/2 or 1/2 states, respectively. For a given temperature, the average $v=0$, $j=0$ rate constant can be evaluated by

$$k_{v=0,j=0}(T)=\frac{4}{4+2e^{-\Delta/k_BT}}k_{v=0,j=0,j_a=3/2}(T)+\frac{2e^{-\Delta/k_BT}}{4+2e^{-\Delta/k_BT}}k_{v=0,j=0,j_a=1/2}(T). \quad (21)$$

At 200 K, the $k_{v=0,j=0}(T)$ is $7.62\times10^{-12}\,cm^3\,s^{-1}$, to be compared with the value of $7.52\times10^{-12}\,cm^3\,s^{-1}$ obtained if only reaction from the 3/2 state would have taken place. The

corresponding rate constants calculated from the excitation functions on the HSW and SW PESs at this temperature are $6.88\times10^{-12}\,cm^3\,s^{-1}$ and $1.60\times10^{-11}\,cm^3\,s^{-1}$, respectively. Thus, the contribution to reaction of the $F(^2P_{1/2})$ spin–orbit excited atoms represents just 1% of the total rate constant. Similar calculations at 300 K show that the contribution of the F-atom excited state is 2% of the total rate constant. In view of the nonadiabatic reaction probabilities for $j=1$ reported in Ref. 39, it can be expected that thermal rate constants will have a somewhat higher participation of the 1/2 state. Notice, however, that at 300 K the contribution of the $F(^2P_{1/2})$ atoms to the total reactivity should be of $\approx 40\%$ to bring the rate constants into agreement with the experimental values.

V. CONCLUSIONS

Accurate and adiabatic rotation approximate (ARA) quantum mechanical calculations of reaction probabilities and cumulative reaction probabilities have been carried out at selected values of the total angular momentum J for the $F+H_2$ reaction on the *ab initio* SW and HSW PESs. The latter PES includes spin–orbit corrections in the entrance channel, whose net effect is to raise the adiabatic barrier by approximately 1/3 of the F-atom spin–orbit splitting with respect to the original SW PES.

A very good accordance between the accurate and ARA cumulative reaction probabilities (CRP) calculated on a given PES has been found for low values of J, and the agreement worsens significantly with growing J due to the increasing importance of the Coriolis coupling. The accurate and ARA CRPs have been employed to obtain ''exact'' and ARA thermal rate constants by linear interpolations, which have been found in good agreement in spite of the discrepancies observed in the CRPs at high J values. In addition, the J-shifting approximation has been employed to calculate rate constants from the accurate CRPs at $J=0$ and $J=1$ (hereafter JSA0 and JSA1 $k(T)$'s, respectively). It has been found that the JSA1 $k(T)$'s are in much better agreement with the ''exact'' and ARA $k(T)$'s than the JSA0 ones.

The availability of the HSW PES, which includes spin–orbit coupling effects in the entrance channel, has allowed the verification of the correction proposed recently by Matzkies and Manthe [40] in the electronic partition function of the reagent with spin–orbit splitting. This correction accounts for the spin–orbit coupling in a PES involving open-shell atoms or molecules constructed without taking into account such interaction, as it is the case of the SW PES. It has been found that the rate constants calculated on the HSW PES coincide very precisely with those calculated on the SW PES by applying the correction in the electronic partition function. From the comparison of the adiabatic rate constants on both PESs, it has been demonstrated that the inclusion of the spin–orbit coupling on the potential surface leads to a significant decrease in the magnitude of the rate constants, which, in addition, have found to be systematically smaller than the experimental determinations. Therefore, when spin–orbit effects are taken into account, the barrier of the PES is too high to account for the experimental measurements.

An estimate of the participation of the $F(^2P_{1/2})$ spin–orbit excited atoms to the rate constants through nonadiabatic channels, by using the J-shifting approximation from the reaction probabilities calculated nonadiabatically by Alexander *et al.*[39] has proven to be very small and uncapable of resolving the discrepancies between the theoretical and experimental rate coefficients.

Since the molecular beam experiments are better accounted for by QM scattering calculations on the SW PES than on the spin–orbit corrected HSW PES,[31] it must be concluded that the size of the actual barrier of the surface with spin–orbit effects included should be very near to that found in the original adiabatic SW PES.

ACKNOWLEDGMENTS

We are indebted to Professor Millard H. Alexander for sending us the QM results of Ref. 39. J.F.C. acknowledges finantial support through the program ''Acciones para la Incorporación de Doctores *y* Tecnólogos'' from the Ministry of Education and Culture of Spain. This work was financed by the DGICYT of Spain under Project No. PB95-0918-C03.

[1] D. E. Manolopoulos, J. Chem. Soc., Faraday Trans. **93**, 673 (1997), and references therein.
[2] F. J. Aoiz, L. Bañares, and V. J. Herrero, J. Chem. Soc., Faraday Trans. **94**, 2483 (1998).
[3] F. J. Aoiz, L. Bañares, and V. J. Herrero, in *Advances in Classical Trajectory Methods*, edited by W. Hase (JAI, Connecticut, 1998), Vol. 3, pp. 121–182.
[4] D. M. Neumark, A. M. Wodtke, G. N. Robinson, C. C. Hayden, and Y. T. Lee, J. Chem. Phys. **82**, 3045 (1985).
[5] D. M. Neumark, A. M. Wodtke, G. N. Robinson, C. C. Hayden, R. Shobatake, R. K. Sparks, T. P. Schafer, and Y. T. Lee, J. Chem. Phys. **82**, 3067 (1985).
[6] R. D. Levine and R. B. Bernstein, *Molecular Reactions Dynamics and Chemical Reactivity* (Oxford University Press, Oxford, 1987).
[7] D. A. McQuarrie and J. D. Simon, *Physical Chemistry. A Molecular Approach* (University Science Books, Sausalito, 1997).
[8] M. Brouard, *Reaction Dynamics* (Oxford University Press, Oxford, 1998).
[9] M. Faubel, L. Y. Rusin, F. Sondermann, S. Schlemmer, U. Tappe, and J. P. Toennies, J. Chem. Phys. **101**, 2106 (1994).
[10] M. Faubel, B. Martínez-Haya, L. Y. Rusin, U. Tappe, and J. P. Toennies, Chem. Phys. Lett. **232**, 197 (1995).
[11] M. Faubel, B. Martínez-Haya, L. Y. Rusin, U. Tappe, J. P. Toennies, F. J. Aoiz, and L. Bañares, Chem. Phys. **207**, 227 (1996).
[12] M. Baer, M. Faubel, B. Martínez-Haya, L. Y. Rusin, U. Tappe, J. P. Toennies, K. Stark, and H.-J. Werner, J. Chem. Phys. **104**, 2743 (1996).
[13] M. Faubel, B. Martínez-Haya, L. Y. Rusin, U. Tappe, and J. P. Toennies, J. Phys. Chem. A **101**, 6415 (1997).
[14] M. Baer, M. Faubel, B. Martínez-Haya, L. Y. Rusin, U. Tappe, and J. P. Toennies, J. Chem. Phys. **108**, 9694 (1998).
[15] M. Faubel, B. Martínez-Haya, L. Y. Rusin, U. Tappe, J. P. Toennies, F. J. Aoiz, and L. Bañares, J. Phys. Chem. A **102**, 8695 (1998).
[16] S. E. Bradforth, D. W. Arnold, D. M. Neumark, and D. E. Manolopoulos, J. Chem. Phys. **99**, 6345 (1993).
[17] D. E. Manolopoulos, K. Stark, H.-J. Werner, D. W. Arnold, S. E. Bradforth, and D. M. Neumark, Science **262**, 1852 (1993).
[18] W. B. Chapman, B. W. Blackmon, and D. J. Nesbitt, J. Chem. Phys. **107**, 8193 (1997).
[19] W. B. Chapman, B. W. Blackmon, S. Nizkorodov, and D. J. Nesbitt, J. Chem. Phys. **109**, 9306 (1998).
[20] G. Dharmasena, T. R. Phillips, K. N. Shokhirev, G. A. Parker, and M. Keil, J. Chem. Phys. **106**, 9950 (1997).
[21] G. Dharmasena, K. Copeland, J. H. Young, R. A. Lasell, T. R. Phillips, G. A. Parker, and M. Keil, J. Phys. Chem. A **101**, 6429 (1997).
[22] G. C. Lynch, R. Steckler, D. W. Schwenke, A. J. C. Varandas, and D. G. Truhlar, J. Chem. Phys. **94**, 7136 (1991).

[23] S. L. Mielke, G. C. Lynch, D. G. Truhlar, and D. W. Schwenke, Chem. Phys. Lett. **213**, 11 (1993); **217**, 173E (1994).
[24] K. Stark and H.-J. Werner, J. Chem. Phys. **104**, 6515 (1996).
[25] J. F. Castillo, D. E. Manolopoulos, K. Stark, and H.-J. Werner, J. Chem. Phys. **104**, 6531 (1996).
[26] J. F. Castillo and D. E. Manolopoulos, Faraday Discuss. Chem. Soc. **110**, 119 (1998). See also the General Discussion in this issue.
[27] F. J. Aoiz, L. Bañares, V. J. Herrero, V. Sáez Rábanos, K. Stark, and H.-J. Werner, Chem. Phys. Lett. **223**, 215 (1994).
[28] F. J. Aoiz, L. Bañares, V. J. Herrero, V. Sáez Rábanos, K. Stark, and H.-J. Werner, J. Phys. Chem. **98**, 10665 (1994).
[29] F. J. Aoiz, L. Bañares, V. J. Herrero, V. Sáez Rábanos, K. Stark, and H.-J. Werner, J. Chem. Phys. **102**, 9248 (1995).
[30] F. J. Aoiz, L. Bañares, B. Martínez-Haya, J. F. Castillo, D. E. Manolopoulos, K. Stark, and H.-J. Werner, J. Phys. Chem. **101**, 6403 (1997).
[31] J. F. Castillo, B. Hartke, H.-J. Werner, F. J. Aoiz, L. Bañares, and B. Martínez-Haya, J. Chem. Phys. **109**, 7224 (1998).
[32] A. Persky and H. Kornweitz, Int. J. Chem. Kinet. **29**, 67 (1997).
[33] E. Wurzberg and P. L. Houston, J. Chem. Phys. **72**, 4811 (1980).
[34] R. F. Heidner, J. F. Bott, C. E. Gardner, and J. E. Melzer, J. Chem. Phys. **72**, 4815 (1980).
[35] P. S. Stevens, W. H. Brune, and J. G. Anderson, J. Phys. Chem. **93**, 4068 (1989).
[36] E. Rosenman, S. Hochman-Kowal, A. Persky, and M. Baer, Chem. Phys. Lett. **257**, 421 (1996).
[37] H. Wang, W. H. Thompson, and W. H. Miller, J. Phys. Chem. A **102**, 9372 (1998).
[38] B. Hartke and H.-J. Werner, Chem. Phys. Lett. **280**, 430 (1997).
[39] M. H. Alexander, H.-J. Werner, and D. E. Manolopoulos, J. Chem. Phys. **109**, 5710 (1998).
[40] F. Matzkies and U. Manthe, J. Chem. Phys. **108**, 4828 (1998).
[41] H. Wang, W. H. Thompson, and W. H. Miller, J. Chem. Phys. **107**, 7194 (1997).
[42] M. P. de Miranda, D. C. Clary, J. F. Castillo, and D. E. Manolopoulos, J. Chem. Phys. **108**, 3142 (1998).
[43] E. Wrede, L. Schnieder, K. H. Welge, F. J. Aoiz, L. Bañares, J. F. Castillo, B. Martínez-Haya, and V. J. Herrero, J. Chem. Phys. **110**, 9971 (1999).
[44] J. M. Bowman, Adv. Chem. Phys. **61**, 115 (1985).
[45] G. Herzberg, *Molecular Spectra and Molecular Structure. II Infrared and Raman Spectra of Poliatomic Molecules* (Van Nostrand Reinhold, New York, 1979).
[46] D. Wang and J. M. Bowman, J. Phys. Chem. **98**, 7994 (1994).
[47] S. L. Mielke, G. C. Lynch, D. G. Truhlar, and D. W. Schwenke, Chem. Phys. Lett. **216**, 441 (1993).
[48] G. C. Schatz, P. McCabe, and J. N. L. Connor, Faraday Discuss. **110**, 139 (1998).
[49] J. M. Bowman, Chem. Phys. Lett. **217**, 36 (1994).
[50] D. de Fazio and J. F. Castillo, Phys. Chem. Chem. Phys. **1**, 1165 (1999), and references therein.
[51] D. C. Chatfield, R. S. Friedman, D. G. Truhlar, B. C. Garret, and D. W. Schwenke, J. Am. Chem. Soc. **113**, 486 (1991).
[52] D. C. Chatfield, R. S. Friedman, D. W. Schwenke, and D. G. Truhlar, J. Phys. Chem. **96**, 2414 (1992).
[53] J. F. Castillo (unpublished).